Pergamon

0094-114X(94)00052-2

Mech. Mach. Theory Vol. 30, No. 4, pp. 533–551, 1995

0094-114X/95 $9.50 + 0.00

ON THE QUADRATIC NATURE OF THE SINGULARITY CURVES OF PLANAR THREE-DEGREE-OF-FREEDOM PARALLEL MANIPULATORS

JAOUAD SEFRIOUI and CLÉMENT M. GOSSELIN
Département de Génie Mécanique, Université Laval, Ste-Foy, Québec, Canada G1K 7P4

(Received 1 December 1993; received for publication 1 September 1994)

Abstract—In this paper, the singularity loci of general three-degree-of-freedom planar parallel manipulators are studied and a graphical representation of these loci in the manipulator's workspace is obtained. The algorithm used here is based on the determination of the roots of the determinant of the manipulator's Jacobian matrix. As mentioned elsewhere, two different types of singularities can occur when parallel manipulators are actuated. Both types are considered here and it is shown that one of the two types leads to a trivial description while the second one is more challenging. On the other hand, architectural singularities are not considered since they are assumed to be eliminated from the outset by a proper choice of the kinematic parameters. Indeed, for the type of manipulator studied here, architectural singularities are very easy to predict and were studied in detail elsewhere. Analytical expressions describing the singularity locus of a planar parallel manipulator are obtained here. Moreover, it is shown that, for a given orientation of the platform, the singularity locus in the plane of motion is a quadratic form, i.e., either a hyperbola, a parabola or an ellipse. Examples illustrating these results are given. For each of these examples, the corresponding singularity locus is graphically superimposed on the manipulator's workspace. This feature has been included in a package developed for the CAD of parallel manipulators. Cases of manipulators for which the singularity locus is located outside of the workspace for certain orientations of the platform are presented. Additionally, three-dimensional represention of the singularity loci are given. The graphical representation of the singularity loci is a very powerful design tool which can be of great help, especially in the context of parallel manipulators.

INTRODUCTION

The diversity of potential applications for advanced robotic manipulators has stimulated the proliferation of various ideas for the design of specialized robotic devices. One of the avenues that has been investigated by researchers over the past decade is the design of robotic manipulators having a parallel mechanical architecture (see for instance [1–8]). Parallel manipulators, as they are referred to, can offer better structural rigidity, kinematic accuracy and dynamic properties. On the other hand, they generally have a rather limited workspace. Additionally, they are known to lead to a special type of local degeneracy which is a property of closed kinematic chains. This type of singularity has been mentioned by most of the researchers working on parallel manipulators as a potential difficulty to be carefully addressed. In [9], a systematic classification of all types of singularities that can occur for parallel manipulators has been presented. This work has been complemented in [10] where architecture singularities are studied in more detail.

In this paper, the singularities of planar three-degree-of-freedom parallel manipulators will be studied. As shown in [9], architecture singularities are well known and easily avoided for this type of manipulator. Moreover, singularities of type I—following the classification given in the latter reference—are known to happen at the boundary of the Cartesian workspace, which in turn can be obtained from the algorithm described in [11]. Hence, we will focus on the second type of local degeneracy—singularities of type II in [9]—which are more elusive to geometric analyses. Physically, these configurations lead to: (i) an instantaneous change in the degree-of-freedom of the system and hence a loss of the controllability, and (ii) an important degradation of the natural stiffness which may lead to very high joint forces or torques. Therefore, it is very important to be able to identify singular configurations at the design stage in order to improve the system's performance. In [12], singularities of this type have been studied for a spatial six-degree-of-freedom parallel manipulator using Grassmann geometry. This led to an exhaustive list of geometric conditions under which such singularities are encountered. However, from a design point of view,

it is desirable to develop a tool that will allow to determine easily the locus of singular configurations in the manipulator's Cartesian workspace. In other words, given a set of design parameters, provide the designer with a representation of the singularity locus. Such a result cannot be achieved with geometrical methods.

The approach used here consists in obtaining analytical expressions for the determinant of the Jacobian matrix. These expressions are then used to construct the singularity loci. In this paper, such expressions have been obtained for planar three-degree-of-freedom parallel manipulators with general architecture. This work generalizes the results presented in [13] for particular architectures. It is shown here that, for a given orientation of the platform, the singularity locus in the Cartesian space is a curve of degree 2 which can be either a hyperbola, an ellipse or a parabola, depending on the geometric parameters of the robot and of the orientation chosen. An interactive graphical tool has been developed and included in a CAD package written specifically for parallel manipulators. This tool can be very helpful for the designer by allowing the superposition of the singularity locus and the workspace. Examples of results obtained with the package are presented in the paper.

In order to clearly illustrate the approach, the analysis for a simple two-degree-of-freedom closed-loop manipulator will first be presented. In this case, the singularity loci and their physical interpretation will be very easy to derive and will provide more insight into the problem. Planar three-degree-of-freedom parallel manipulators will then be treated.

SINGULARITY ANALYSIS

Let $\boldsymbol{\theta}$ and $\mathbf{x}$ be the vector of joint coordinates and the vector of Cartesian coordinates of the n degree-of-freedom parallel manipulator, respectively. In terms of components, $\boldsymbol{\theta}$ and $\mathbf{x}$ can be written as:

$$\boldsymbol{\theta} = [\theta_1, \theta_2, \ldots, \theta_n]^{\mathrm{T}}$$

$$\mathbf{x} = [x_1, x_2, \ldots, x_n]^{\mathrm{T}}$$

where θ_i is the variable associated with the displacement of a prismatic joint or with the rotation of a revolute joint. Similarly, x_i is a component of a position or an orientation in the Cartesian space. Vectors $\boldsymbol{\theta}$ and $\mathbf{x}$ are also respectively called the input and output variables of the manipulator. They are related by the nonlinear kinematic constraints which can be expressed as the following vector equation:

$$\mathbf{F}(\boldsymbol{\theta}, \mathbf{x}) = \mathbf{0} \tag{1}$$

where $\mathbf{0}$ is the n-dimensional zero vector. Differentiating equation (1) with respect to time, one obtains

$$\mathbf{A}\dot{\mathbf{x}} + \mathbf{B}\dot{\boldsymbol{\theta}} = \mathbf{0} \tag{2}$$

where

$$\mathbf{A} = \frac{\partial \mathbf{F}}{\partial \mathbf{x}} \tag{3}$$

$$\mathbf{B} = \frac{\partial \mathbf{F}}{\partial \boldsymbol{\theta}} \tag{4}$$

and where $\mathbf{A}$ and $\mathbf{B}$ are n-dimensional square matrices which are configuration dependent. These matrices are called Jacobian matrices.

In [9], Gosselin and Angeles have suggested a classification of the different types of singularities encountered in closed kinematic chains by considering the Jacobian matrices $\mathbf{A}$ and $\mathbf{B}$ defined above. They have identified three types of singularities, each having a different physical interpretation. This classification is now repeated:

1. Singularity of type I: occurs when matrix $\mathbf{B}$ is singular
2. Singularity of type II: occurs when matrix $\mathbf{A}$ is singular
3. Singularity of type III: occurs when the nonlinear kinematic constraints degenerate.

In this paper the singularity loci associated with the singularities of type I and II of the planar three-degree-of-freedom parallel manipulator are studied. The third type of singularity will be assumed to be avoided by a proper choice of the kinematic parameters. In fact, the conditions under which this type of singularity can occur for a planar parallel manipulator are well known [9] and can be easily avoided.

An example presenting the analysis of a simple two-degree-of-freedom mechanism will now be presented in order to clearly describe the algorithm used to obtain the singularity loci. Three-degree-of-freedom parallel manipulators will then be introduced.

Planar two-degree-of-freedom RPRPR mechanism

This 5-bar mechanism is represented in Fig. 1. It consists of two active prismatic joints and three passive revolute joints, forming one closed-loop.

By controlling the displacement of the prismatic joints, i.e., the length of each of the legs ρ_1 and ρ_2, point M can be positioned arbitrarily in the plane.

Inverse kinematics. The inverse kinematics of this simple 2-dof device is rather trivial. Indeed, given the desired position of point M, the lengths of the legs are computed as:

$$\rho_1 = \sqrt{x^2 + y^2} \tag{5}$$

$$\rho_2 = \sqrt{(x-a)^2 + y^2} \tag{6}$$

Therefore, the inverse kinematics of this mechanism admits a unique solution.

Direct kinematics. Given the values of the joint coordinates ρ_1 and ρ_2, the position of point M denoted by the two components (x, y), can be obtained by solving equations (5, 6) for x and y. This leads to

$$x = \frac{\rho_1^2 - \rho_2^2}{2a} \tag{7}$$

$$y = \pm\sqrt{\rho_1^2 - \left(\frac{\rho_1^2 - \rho_2^2}{2a}\right)^2} \tag{8}$$

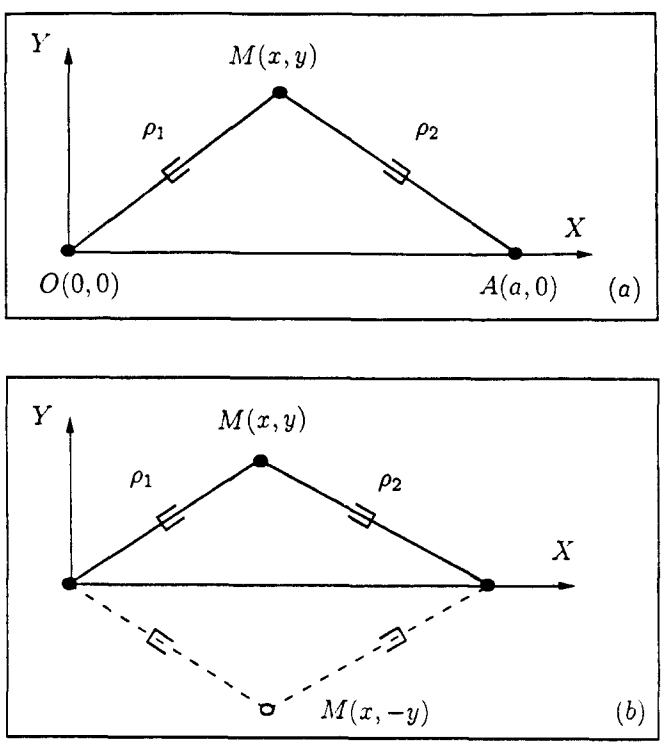

Fig. 1. (a) Planar *RPRPR* mechanism, (b) the two assembly modes.

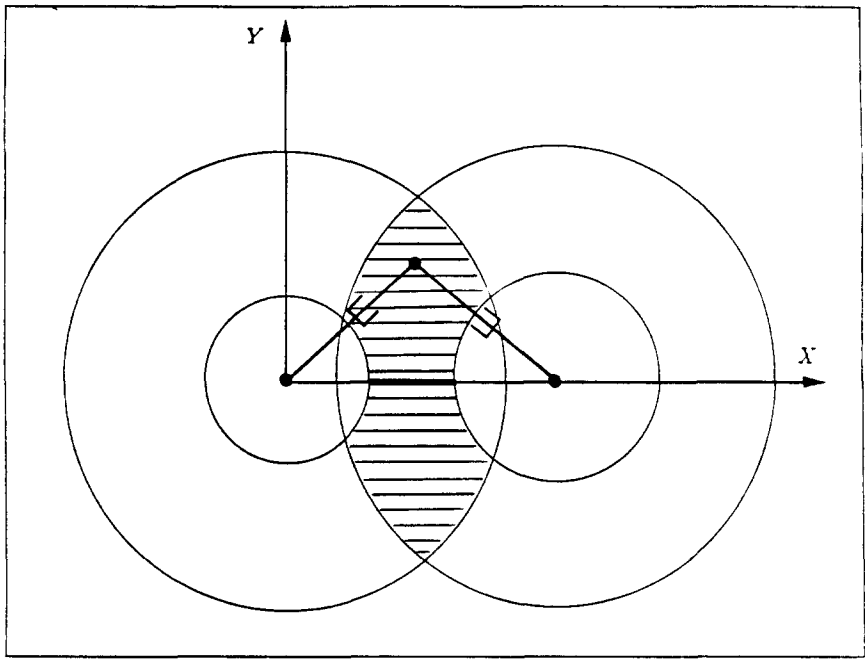

Fig. 2. Cartesian workspace of the *RPRPR* mechanism.

As opposed to the inverse one, the direct kinematic problem leads to a maximum of 2 solutions. The two branches obtained are symmetric with respect to the X axis since the sign indetermination appears only in the solution for y [Fig. 1(b)].

Workspace. The Cartesian workspace of this mechanism is bounded by the set of configurations for which one of the prismatic joints reaches one of its limits. If we denote the minimum and the maximum value of the joint variables by $\rho_{i,\min}$ and $\rho_{i,\max}$, respectively, it is readily observed that the workspace is given by the intersection of two annular regions. These regions are centered at points O and A, respectively, and each of these regions is bounded by two concentric circles of radii $\rho_{i,\min}$ and $\rho_{i,\max}$. This is represented in Fig. 2.

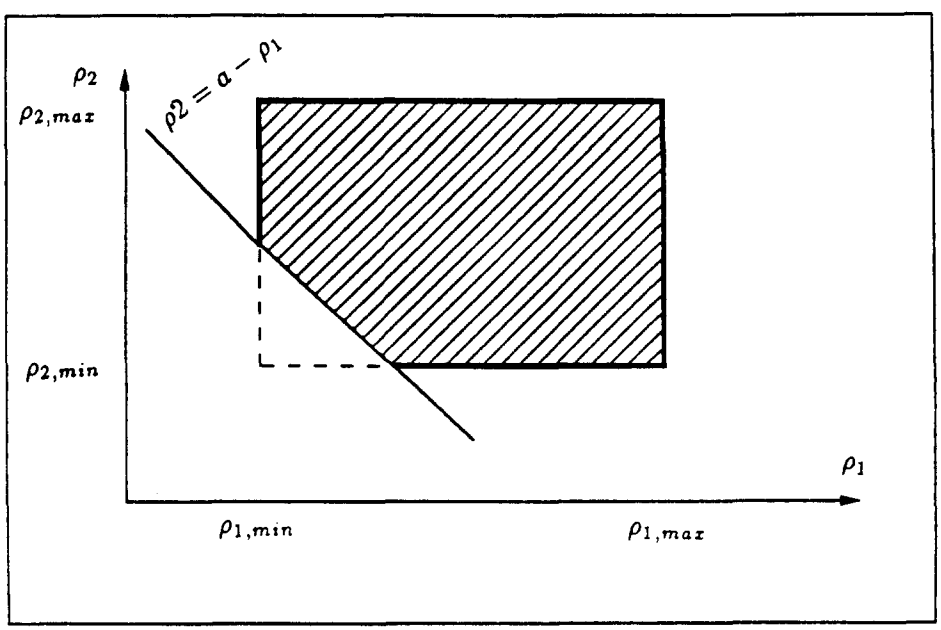

Fig. 3. Workspace for the *RPRPR* mechanism in the joint space.

As shown in [9], the singularities of type I will occur at the boundary of the Cartesian workspace. A representation of the workspace in the joint space is given in Fig. 3. It is obtained by noticing that each of the joint variables is limited by two extreme values and that the following constraint, i.e.,

$$\rho_1 + \rho_2 \geqslant a$$

must be satisfied for the mechanism to be assembled.

Singularity analysis. Differentiating equations (5) and (6) with respect to time leads to:

$$\mathbf{A}\dot{\mathbf{x}} + \mathbf{B}\dot{\boldsymbol{\theta}} = \mathbf{0}$$

where

- $\dot{\mathbf{x}} = [\dot{x}, \dot{y}]^T$ is the Cartesian velocity vector and
- $\dot{\boldsymbol{\theta}} = [\dot{\rho}_1, \dot{\rho}_2]^T$ is the joint velocity vector.

and where **A** and **B** are the Jacobian matrices which can be expressed as:

$$\mathbf{A} = \begin{bmatrix} x & y \\ x - a & y \end{bmatrix} \quad \text{and} \quad \mathbf{B} = \begin{bmatrix} \rho_1 & 0 \\ 0 & \rho_2 \end{bmatrix}$$

(a) Singularity loci for singularities of type I

The configurations corresponding to singularities of type I are the ones for which

$$\det(\mathbf{B}) = 0$$

i.e.

$$\rho_1 = 0 \quad \text{or} \quad \rho_2 = 0$$

However, in a real situation, ρ_1 and ρ_2 cannot be equal to zero. Physically, this type of singularity will occur when either ρ_1 or ρ_2 reaches one of its limits. It is noted that this result is obtained from geometric reasoning rather than from a formal mathematical derivation.

The graphical representation of the locus of the singularities of type I is therefore easily obtained. In the Cartesian space (Fig. 2), this locus is the boundary of the workspace since this boundary corresponds to maximum or minimum values of the joint variables. In the joint space (ρ_1, ρ_2), it is represented by the straight lines associated with minimum and maximum values of ρ_1 and ρ_2 and it does not necessarily correspond to the whole boundary of the workspace (Fig. 3).

(b) Singularity loci for singularities of type II

This type of singularity occurs when

$$\det(\mathbf{A}) = 0$$

In the case of this mechanism, we have

$$\det(\mathbf{A}) = ay = 0 \Rightarrow \begin{cases} a = 0 \\ \text{or } y = 0 \end{cases}$$

The first case, i.e. $a = 0$, corresponds to an architecture singularity which can be easily avoided by choosing points O and A distinct. Hence, it is assumed here that $a \neq 0$.

The second case, i.e. $y = 0$, corresponds to the singularities of type II. These configurations occur when point M is located on the X axis, i.e., on the line connecting points O and A. The representation of the locus for this type of singularity in the Cartesian space is represented in Fig. 2. It consists of a segment on the X axis breaking the workspace in two symmetric regions. Clearly, this type of singularity can be avoided if the value of the geometric parameter a is chosen such that it verifies the following inequality:

$$a < \rho_{1\min} + \rho_{2\min}$$

This is illustrated in Fig. 4 where a mechanism of this type is shown.

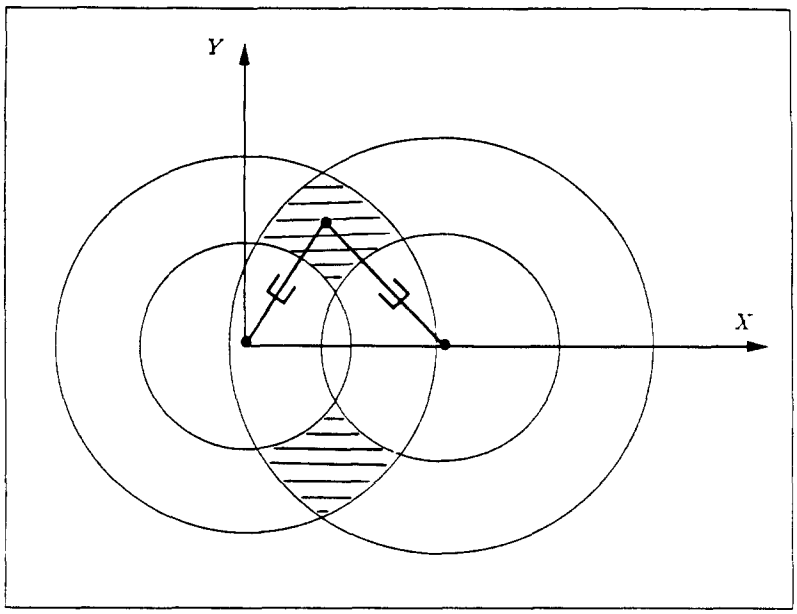

Fig. 4. Planar *RPRPR* mechanism with no type II singularity.

In the joint space, the locus of the singularities of type II is obtained by the substitution of the joint coordinates in the second condition ($y = 0$). This leads to

$$\rho_1 + \rho_2 = a$$

which is the equation of a straight line, as illustrated in Fig. 3. It is noticed, in this figure, that this locus constitutes a boundary of the workspace in the joint space. In a singular configuration of type II, point M can undergo a nonzero velocity in the direction perpendicular to the X axis even if the velocities of the actuators are equal to zero.

The physical interpretation of the singularities and the loci obtained for the mechanism presented above are quite simple. The objective now is to use the same approach to obtain the singularity loci of planar three-degree-of-freedom parallel manipulators. The locus of the singularities of type I will remain rather simple whereas the locus of the singularities of type II will lead to more complicated expressions. They are developed and analyzed in the next section.

PLANAR THREE-DEGREE-OF-FREEDOM PARALLEL MANIPULATORS

A planar three-degree-of-freedom parallel manipulator is represented in Fig. 5. The three prismatic actuators are mounted on unactuated revolute joints and allow the positioning and the orientation of a platform in a plane. This type of manipulator has been studied in the past (see for instance [14]) and its potential applications include part handling, welding, deburring and milling. It can also be built with revolute actuators, as shown in [14].

Let us first consider the case of a general architecture, as shown in Fig. 5. For this class of manipulator, the direct kinematic problem has been solved using polynomial forms in [15].

Computation of the Jacobian matrices

By inspection of Fig. 5, the inverse kinematic problems is readily solved. Indeed, one has:

$$\rho_1^2 = x^2 + y^2 \tag{9}$$

$$\rho_2^2 = (x + l_2 \cos\phi - c_2)^2 + (y + l_2 \sin\phi)^2 \tag{10}$$

$$\rho_3^2 = [x + l_3 \cos(\phi + \gamma) - c_3]^2 + [y + l_3 \sin(\phi + \gamma) - d_3]^2 \tag{11}$$

where γ, c_2, c_3, d_3, l_2 and l_3 are kinematic parameters which are defined in Fig. 5.

Now let $\mathbf{x} = [x, y, \phi]^T$, be the vector of Cartesian coordinates and $\boldsymbol{\theta} = [\rho_1, \rho_2, \rho_3]^T$, be the vector of joint coordinates. The differentiation of equations (9–11) with respect to time can be written in matrix form as:

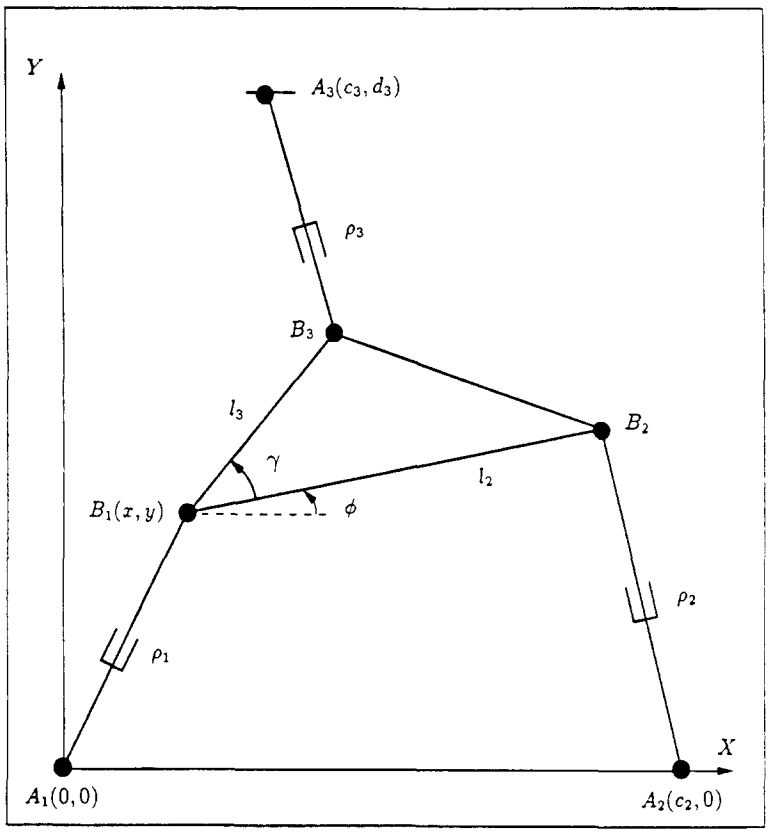

Fig. 5. Planar three-degree-of-freedom parallel manipulator.

$$\mathbf{A}\dot{\mathbf{x}} + \mathbf{B}\dot{\boldsymbol{\theta}} = 0$$

where **A** and **B** are the 3×3 Jacobian matrices. They are written as:

$$\mathbf{A} = \begin{bmatrix} a_{11} & a_{12} & a_{13} \\ a_{21} & a_{22} & a_{23} \\ a_{31} & a_{32} & a_{33} \end{bmatrix} \tag{12}$$

and

$$\mathbf{B} = \begin{bmatrix} \rho_1 & 0 & 0 \\ 0 & \rho_2 & 0 \\ 0 & 0 & \rho_3 \end{bmatrix} \tag{13}$$

with

$$a_{11} = x \tag{14}$$

$$a_{12} = y \tag{15}$$

$$a_{13} = 0 \tag{16}$$

$$a_{21} = (x - c_2) + l_2 \cos\phi \tag{17}$$

$$a_{22} = y + l_2 \sin\phi \tag{18}$$

$$a_{23} = l_2(y \cos\phi - (x - c_2)\sin\phi) \tag{19}$$

$$a_{31} = (x - c_3) + l_3 \cos(\phi + \gamma) \tag{20}$$

$$a_{32} = (y - d_3) + l_3 \sin(\phi + \gamma)$$

$$a_{33} = l_3[(y - d_3)\cos(\phi + \gamma) - (x - c_3)\sin(\phi + \gamma)] \tag{21}$$

Singularities of type I

As stated above, these singularities occur when

$$\det(\mathbf{B}) = 0$$

Mathematically, this condition leads to:

$$\rho_i = 0, \quad i = 1 \quad \text{or} \quad 2 \quad \text{or} \quad 3$$

However, as pointed out in the preceding section, since the prismatic joints do not have an infinite range of motion, this singularity will occur whenever one of the joints reaches one of its limits, i.e., when $\rho_i = \rho_{i,\min}$ or $\rho_{i,\max}$ for $i = 1, 2$ or 3. This is in fact the boundary of the Cartesian workspace.

Singularities of type II

Analytical expression of the singularity locus. Singularities of type II occur when matrix **A** is singular, i.e., when

$$\det(\mathbf{A}) = 0 \tag{22}$$

where **A** is given in equation (12). From equations (12) and (22), the analytical expression for the singularity locus can be written as:

$$E_1 x^2 + E_2 y^2 + E_3 xy + E_4 x + E_5 y = 0 \tag{23}$$

where the coefficients, E_i, $i = 1, 2, \ldots, 5$, are functions of the geometric parameters of the robot and of the orientation of the platform and are given by:

$$E_1 = -(d_3 l_2 \sin\phi) \tag{24}$$

$$E_2 = -(c_3 l_2 \cos\phi) + c_2 l_3 \cos(\phi + \gamma) \tag{25}$$

$$E_3 = d_3 l_2 \cos\phi + c_3 l_2 \sin\phi - c_2 l_3 \sin(\phi + \gamma) \tag{26}$$

$$E_4 = c_2 d_3 l_2 \sin\phi - d_3 l_2 l_3 \cos(\phi + \gamma)\sin\phi - c_2 l_2 l_3 \sin\phi \sin(\phi + \gamma) + c_3 l_2 l_3 \sin\phi \sin(\phi + \gamma) \tag{27}$$

$$E_5 = -[c_2 d_3 l_3 \cos(\phi + \gamma)] + d_3 l_2 l_3 \cos\phi \cos(\phi + \gamma) - c_2 c_3 l_2 \sin\phi + c_2 l_2 l_3 \cos(\phi + \gamma)\sin\phi + c_2 c_3 l_3 \sin(\phi + \gamma) - c_3 l_2 l_3 \cos\phi \sin(\phi + \gamma) \tag{28}$$

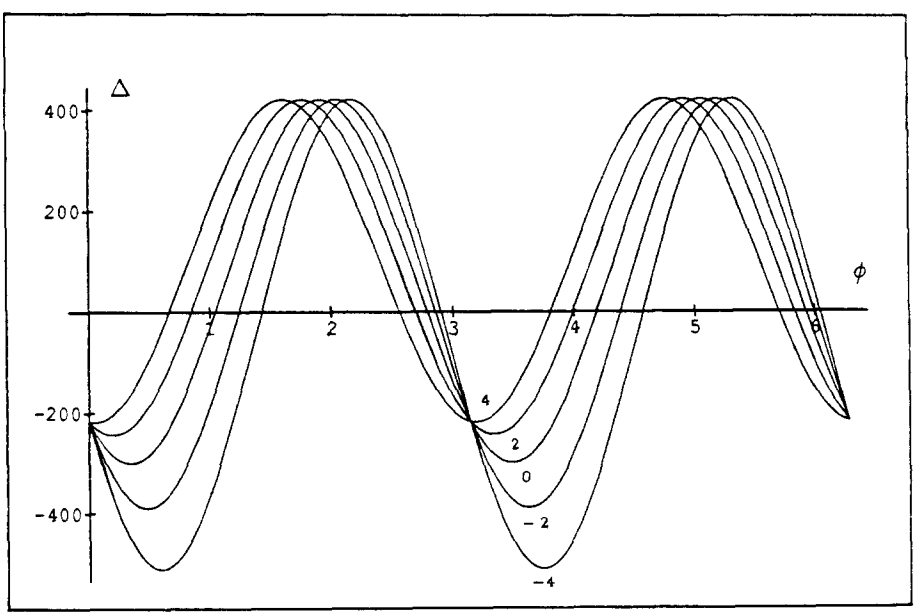

Fig. 6. Variation of Δ as a function of ϕ for different values of c_3 and for $c_2 = 7$, $d_3 = 10$, $l_2 = 4$, $l_3 = 3$ and $\gamma = 30°$.

Identification of the type II singularity locus. For a given orientation of the platform, the singularity locus given here by equation (23) can be thought of as a curve in the (x, y) plane which we will refer to as the singularity curve. For the manipulator under study, this curve has a quadratic form. Moreover, the nature of the curve represented by equation (23) depends on the following quantity [16] (c.f. Appendix A):

$$\Delta = E_1 E_2 - \frac{E_3^2}{4} \tag{29}$$

which can be computed from equations (24–28). This leads to

$$\Delta = A_2 \sin^2 \phi + A_1 \sin \phi \cos \phi + A_0 \tag{30}$$

with

$$A_0 = -(d_3 l_2 - c_2 l_3 \sin \gamma)^2 \tag{31}$$

$$A_1 = 2(c_3 l_2 - c_2 l_3 \cos \gamma)(d_3 l_2 + c_2 l_3 \sin \gamma) \tag{32}$$

$$A_2 = -[(c_3 l_2 - d_3 l_2 - c_2 l_3 \cos \gamma - c_2 l_3 \sin \gamma)(c_3 l_2 + d_3 l_2 - c_2 l_3 \cos \gamma + c_2 l_3 \sin \gamma)] \tag{33}$$

which are coefficients depending on the geometry of the manipulator only.

Since the sign of Δ plays a very important role in the determination of the singularity locus—it will determine the nature of the singularity curve—we will now study its variation under changes in the geometry of the manipulator for different orientations of the platform.

Variation of parameter c_3

A plot of the value of Δ as a function of the orientation of the platform for different values of parameter c_3 is shown in Fig. 6 for given values of the other parameters. It can be realized that this parameter does not have a very important effect on the sign of Δ. For all the curves, Δ can be either positive, in which case the singularity curve is an ellipse, or negative, which will lead to a hyperbola. Moreover, when Δ is equal to zero, the curve is a parabola. Changing the value of c_3 will slightly affect the values of ϕ for which the nature of the curve will change.

Variation of parameter d_3

With parameter c_3 equal to zero, parameter d_3 is now varied, which is equivalent to moving the third fixed unactuated revolute joint along the Y axis (Fig. 5). The results are plotted in Fig. 7. Two different cases are observed:

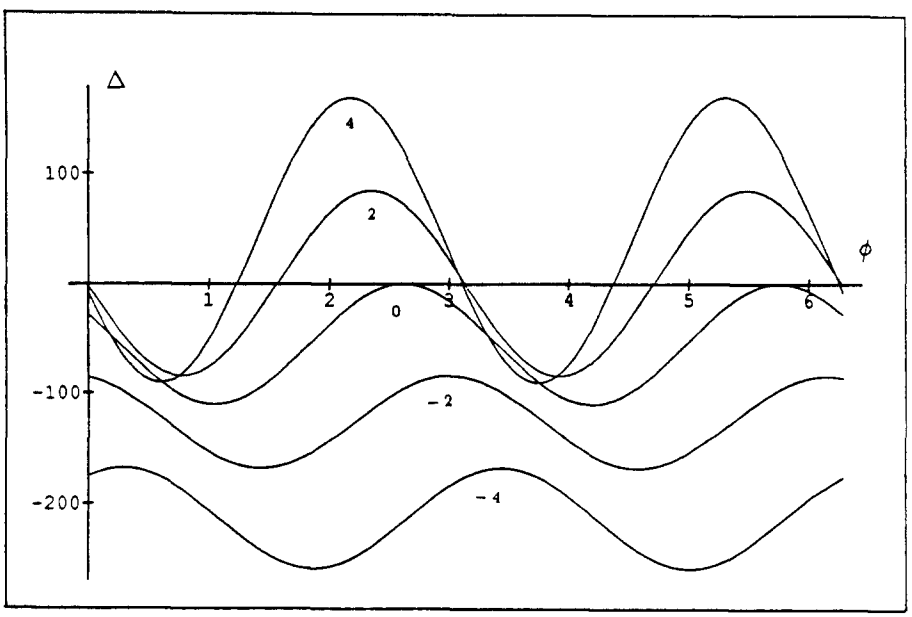

Fig. 7. Variation of Δ as a function of ϕ for different values of d_3 and for $c_2 = 7$, $c_3 = 0$, $l_2 = 4$, $l_3 = 3$ and $\gamma = 30$.

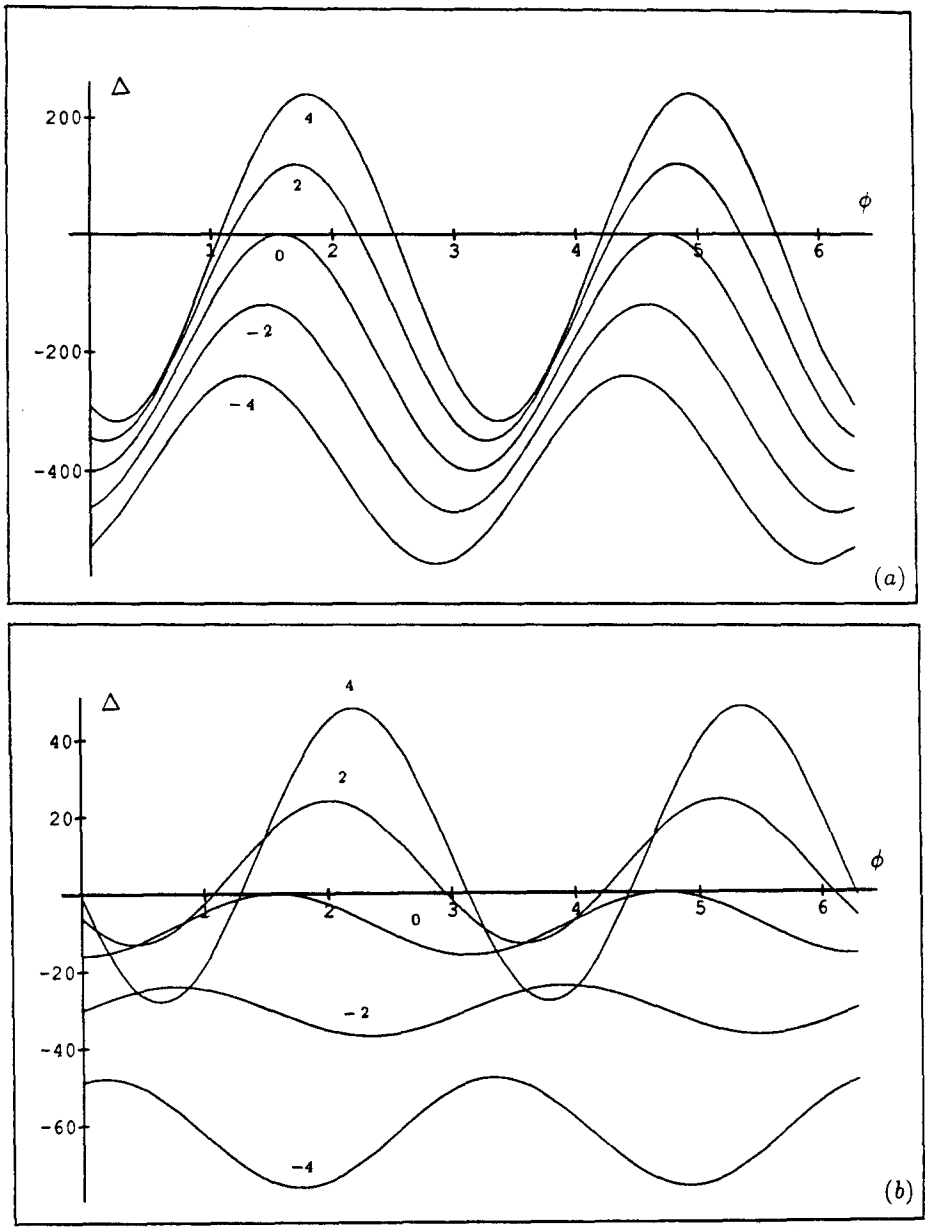

Fig. 8. Variation of Δ as a function of ϕ for different values of c_2 and for $c_3 = 0$, $l_2 = 4$, $l_3 = 3$ and $\gamma = 30°$, with (a) $d_3 = 10$ and (b) $d_3 = -2$.

- $d_3 > 0$ When d_3 is positive, the situation encountered is similar to the one described in the preceding paragraph, i.e., the curve can be either an ellipse, a hyperbola or a parabola depending on the value of the angle of orientation ϕ.
- $d_3 \leqslant 0$ When d_3 is less than or equal to zero, Δ is always negative or equal to zero and, hence, the singularity curve is always a hyperbola—or a parabola for the points for which Δ is equal to zero. This is similar to the case of the simplified manipulator discussed in [13].

Variation of the other parameters

A systematic study of the effect of the other geometric parameters shows that we always get either one of the two cases presented above. Therefore, only a few example curves are now presented. In Figs 8(a) and (b), the effect of parameter c_2 on the value of Δ is investigated for $d_3 > 0$ and $d_3 < 0$, respectively.

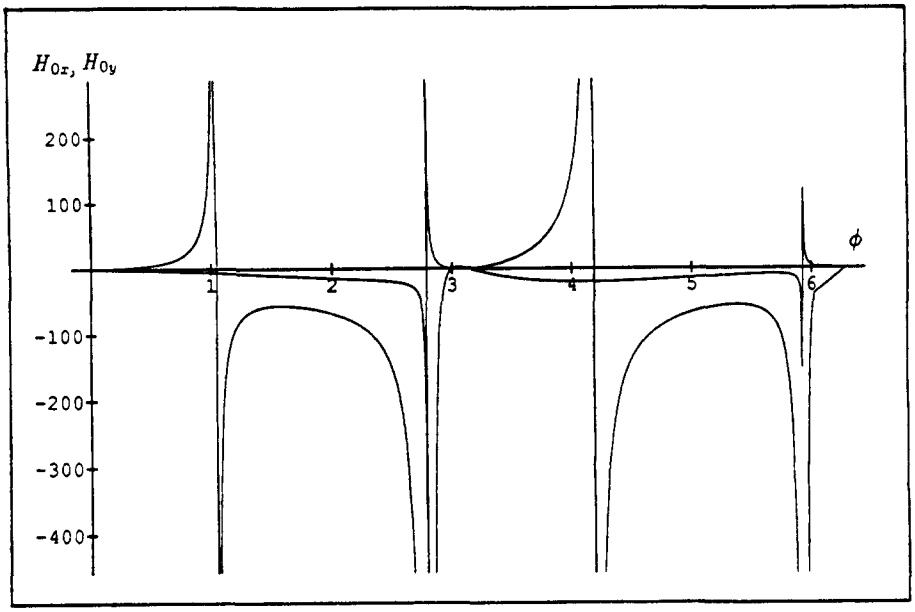

Fig. 9. Variation of the coefficients H_{0x} and H_{0y} as a function of ϕ for $c_2 = 7$, $c_3 = 0$, $d_3 = 10$, $l_2 = 4$, $l_3 = 3$ and $\gamma = 30°$.

In summary, the study of the singularity curves of type II of planar three-degree-of-freedom parallel manipulators leads to two *classes* of manipulators. The first class comprises the manipulators for which the singularity curve is always a hyperbola for any value of the orientation angle ϕ while the manipulators of the second class will lead to a singularity curve that can be either a hyperbola, an ellipse or a parabola depending on the orientation of the platform. These two cases will now be examined in more detail.

Manipulators of the first class

These manipulators are defined as those whose singularity curve of type II will always be a hyperbola, i.e., those for which Δ is always negative, whatever the value of angle ϕ. The analysis presented in [13] is therefore applicable to this case.

Manipulators of the second class

In this case, the value of Δ can either be positive, negative or equal to zero. Therefore, the singularity curve can be an ellipse, a hyperbola or a parabola. For the values of angle ϕ for which Δ is negative, the singularity locus in the XY plane will be a hyperbola. On the other hand, when angle ϕ is equal to ϕ_i, $i = 1, 2, 3$ or 4, the singularity curve will be a parabola since these points correspond to values of ϕ for which Δ is equal to zero. Finally, for the values of ϕ for which Δ is positive, the singularity curve will be an ellipse. Because of the form of the function $\Delta(\phi)$, there will always be 4 values of ϕ which will lead to a parabolic singularity loci. This can be observed in Figs 7, 8(a) and 8(b). In fact, these points are nothing but the roots of $\Delta(\phi) = 0$. The latter equation can be written as

$$A_0 t^4 - 2A_1 t^3 + 2(A_0 + 2A_2)t^2 + 2A_1 t + A_0 = 0 \tag{34}$$

where

$$t = \tan\frac{\phi}{2}$$

and its roots are given as:

$$t_{1,2,3,4} = \frac{\dfrac{A_1}{A_0} \pm D \pm \sqrt{4 + \left(-\dfrac{A_1}{A_0} - D\right)^2}}{2} \tag{35}$$

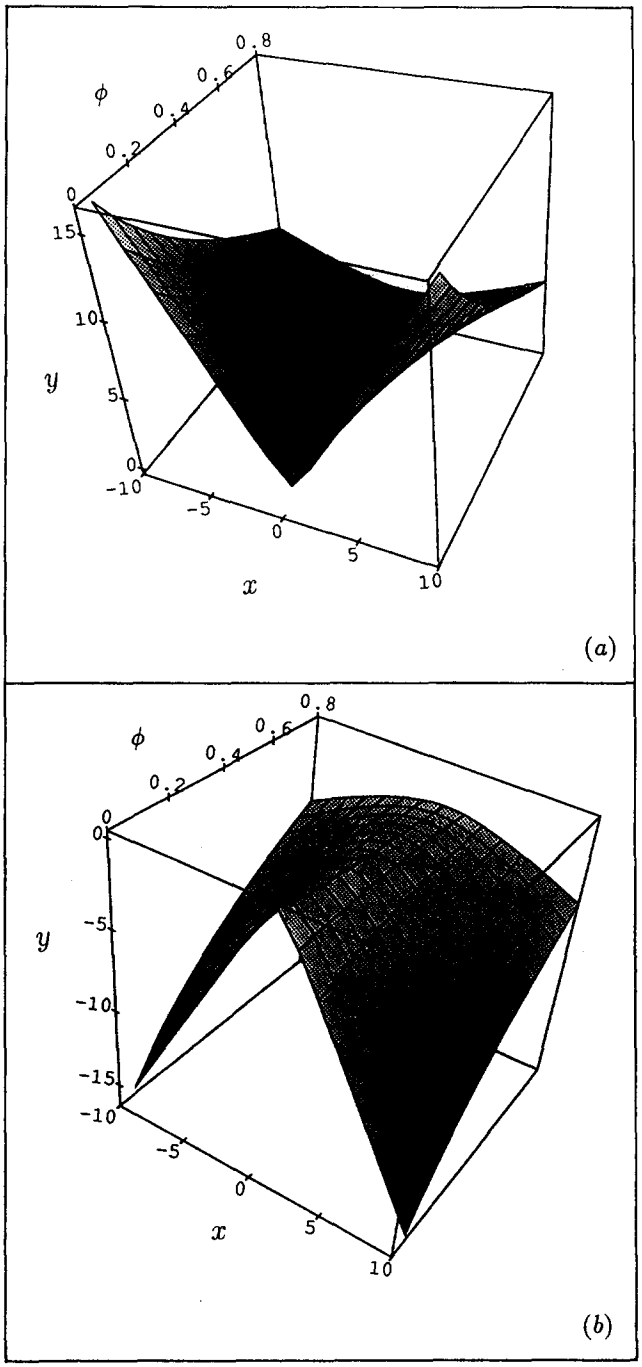

Fig. 10. Three-dimensional singularity locus for a manipulator with $c_2 = 7$, $c_3 = 0$, $d_3 = 10$, $l_2 = 4$, $l_3 = 3$ and $\gamma = 30°$.

with

$$D = \sqrt{-4 + \frac{A_1^2}{A_0^2} - \frac{4A_2}{A_0}}$$

Moreover, we have

$$\Delta(\phi = 0) = A_0 = -(d_3 l_2 - c_2 l_3 \sin\gamma)^2 \leqslant 0 \tag{36}$$

which means that between $\phi = 0$ and $\phi = \phi_1$—the smallest of the roots of equation (34)—the singularity curve is always a hyperbola.

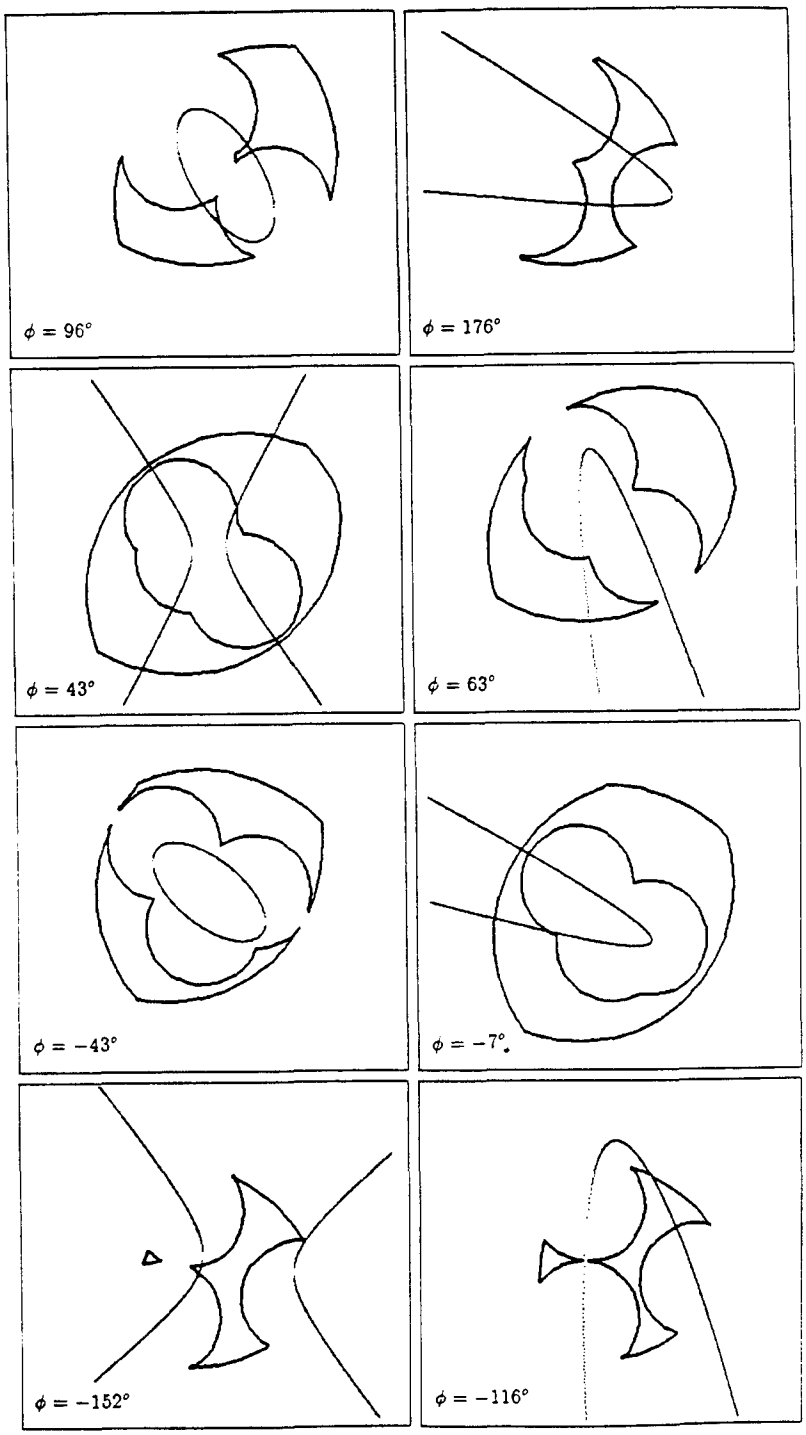

Fig. 11. Superposition of the singularity locus and the workspace for different values of ϕ for a manipulator with $c_2 = 7$, $c_3 = 0$, $d_3 = 6$, $l_2 = 4$, $l_3 = 3$ and $\gamma = 30°$.

Mathematical analysis of the expression of the singularity locus

The planar curve of equation (23) will now be expressed in its principal coordinates in order to determine some of its characteristic and to obtain a three-dimensional representation of the singularities of type II. The details of the procedure are given in Appendix B. The final result is an equation of the form:

$$1 + \frac{X^2}{H_{0x}} + \frac{Y^2}{H_{0y}} = 0 \tag{37}$$

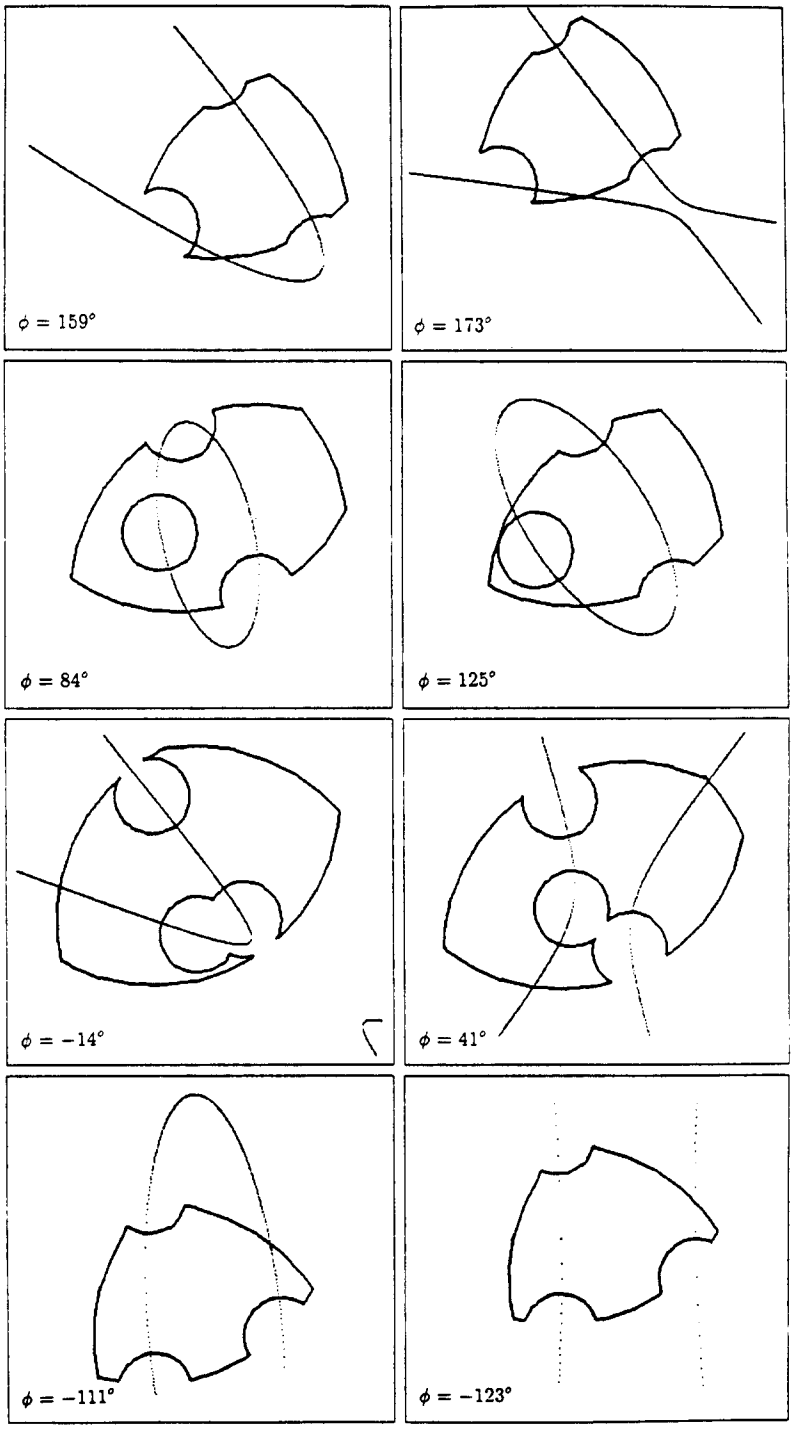

Fig. 12. Superposition of the singularity locus and the workspace for different values of ϕ for a manipulator with $c_2 = 7$, $c_3 = 0$, $d_3 = 10$, $l_2 = 4$, $l_3 = 3$ and $\gamma = 30°$.

where the coefficients H_{0x} and H_{0y} are functions of the geometric parameters of the manipulator and of the orientation of the platform. Expressions for these coefficients are given in Appendix B. In Fig. 9, coefficients H_{0x} and H_{0y} are plotted as a function of the orientation of the platform, ϕ, for a manipulator of the second class having the following geometric parameters:

$$c_2 = 7, \quad c_3 = 0, \quad l_2 = 4, \quad l_3 = 3, \quad d_3 = 10, \quad \gamma = \pi/6$$

It is clear, from Fig. 9, that the two coefficients are sometimes of the same sign and sometimes of opposite signs which means that the singularity curve, equation (37), can be either an ellipse or a hyperbola. Moreover, this curve degenerates into a parabola at the transition points. A three-dimensional representation of the singularity locus—a surface in the (x, y, ϕ) space—is given in Figs 10(a) and 10(b) for the interval of angle ϕ for which the singularity curve is a hyperbola. The two branches of the hyperboloid are represented separately for purposes of clarity.

Superposition of the singularity locus and the workspace of the manipulator

One of the main objectives of the derivations presented in this paper was to include the expressions describing the singularity loci in a package aimed at the computer aided design of parallel manipulators. Such a package—called SIMPA, which stands for *Simulation Interactive de Manipulateurs Parallèles*—has been developed at Laval [17]. The analytical expressions of the singularity loci obtained above have been included in it in order to be able to plot the singularity curves and to superimpose them on the workspace of the manipulator. This feature is of great help to the designer since it allows him to get a very clear picture of the location of the singular configurations of type II in the workspace of the manipulator. (It is recalled that the singularities of type I are simply located at the boundary of the Cartesian workspace).

A few examples of the graphical results obtained with our computer package, SIMPA, are given in Figs 11 and 12. In order to get a very good mobility region for all the orientations of the platform, the legs have been given a range of motion between 2.5 and 7.5 units of length. The geometric parameters of the manipulator used to generate the plots of Fig. 11 are

$$c_2 = 7, \quad c_3 = 0, \quad l_2 = 4, \quad l_3 = 3, \quad d_3 = 6, \quad \gamma = \pi/6$$

and the plots are given for the following orientations of the platform:

$$\phi = \{176^\circ, 96^\circ, 63^\circ, 43^\circ, -7^\circ, -43^\circ, -116^\circ, -152^\circ\}$$

In Fig. 12, the plots have been obtained for a manipulator whose geometric parameters are

$$c_2 = 7, \quad c_3 = 0, \quad l_2 = 4, \quad l_3 = 3, \quad d_3 = 10, \quad \gamma = \pi/6$$

and for orientations of:

$$\phi = \{173^\circ, 159^\circ, 125^\circ, 84^\circ, 41^\circ, -14^\circ, -123^\circ, -111^\circ\}$$

These values of the angle of orientation of the platform have been chosen to illustrate the different types of curves obtained, i.e., hyperbolas, ellipses and parabolas. However, it is recalled that the curves included here have been chosen for purposes of demonstration and that the designer using SIMPA can choose arbitrarily the curves to be plotted. For example, in Fig. 11, cases for which the singularity locus is located outside of the workspace are observed. This type of result is particularly interesting since it means that for the given orientation, the manipulator cannot be in a singular configuration of type II.

CONCLUSION

Analytical expressions describing the singularity loci of planar three-degree-of-freedom parallel manipulators have been obtained in this paper. These expressions have been used to obtain plots of the singularity curves superimposed on the workspace of the manipulator. First of all, the two types of degeneracies that can occur with parallel manipulators have been recalled. As shown elsewhere, the first type of degeneracy is located at the boundary of the Cartesian workspace and can be obtained easily. Therefore, the derivations presented here have focused on the second type of degeneracy. The equations have been obtained by imposing the vanishing of the determinant of one of the Jacobian matrices of the manipulator. It has been shown that, in general, the curve obtained in the XY plane, i.e., for a given value of the orientation of the platform, is a quadratic curve which can be either a hyperbola, an ellipse or a parabola. A class of manipulators for which the singularity locus is always a hyperbola has also been identified. Moreover, three-dimensional representations of the singularity locus have also been obtained, considering the angle of orientation ϕ as the third coordinate. The graphical superposition of the singularity locus and the

Cartesian workspace, which has been implemented in a CAD package dedicated to parallel manipulators, is of great interest in the context of design since it allows the prediction of singular configurations and hence leads to a better optimization of the performance of the system.

Acknowledgements—This work was completed under research grants to the second author from the Natural Sciences and Engineering Research Council of Canada (NSERC) and le Fonds pour la Formation des Chercheurs et l'aide à la Recherche (FCAR) of Québec. The authors also wish to acknowledge the help of Simon Laverdière and Martin Jean who wrote and implemented the software allowing the graphical representation of the singularity loci.

REFERENCES

1. H. MacCallion and D. T. Pham, *Proc. of the 5th World Congress on Theory of Machines and Mechanisms*. Montréal, July (1979).
2. K. H. Hunt, *ASME J. Mech. Transmissions Autom. Design* **105,** 705–712 (1983).
3. D. C. H. Yang and T. W. Lee, *ASME J. Mech. Transmissions Autom. Design* **106,** 191–198 (1984).
4. M. G. Mohamed and J. Duffiy, *ASME J. Mech. Transmissions Autom. Design* **107,** 226–229 (1985).
5. H. Inoue, Y. Tsusaka and T. Fukuizumi, *Proc. of the 3rd Int. Symp. on Robotics Research*, 7–11 October, Gouvieux, France, pp. 321–327 (1985).
6. E. F. Fichter, *The Int. J. Robotics Res.* **5,** 157–182 (1986).
7. J. P. Merlet, *Les Robots Parallèles*. Traité des nouvelles Technologies, Série Robotique, Hermes, France (1990).
8. C. Gosselin, Ph.D. Thesis, McGill University, Montréal, Québec, Canada (1988).
9. C. Gosselin and J. Angeles. *IEEE Trans. Robotics Automn.* **6,** 281–290 (1990).
10. O. Ma and J. Angeles, *Proc. of the IEEE Int. Conf. on Robotics and Automation*, Sacramento, Calif. (1991).
11. C. Gosselin, *ASME J. Mech. Design* **112,** 331–336 (1990).
12. J. P. Merlet, *The Int. J. Robotics Res.* **8,** 45–56 (1989).
13. J. Sefrioui and C. Gosselin, *J. Robotics Autonomous Systems* **10,** 209–224 (1993).
14. C. Gosselin and J. Angeles, *ASME J. Mech. Transmissions Autom. Design* **110,** 35–41 (1988).
15. C. Gosselin and J. Sefrioui, *Proc. of the Fifth Int. Conf. on Advanced Robotics*, Pisa, Italy, pp. 1124–1129 (1991).
16. A. C. Jones, *Introduction to Algebraical Geometry*. Oxford Univ. Press (1912).
17. C. Gosselin, S. Laverdière and J. Côté, *Proc. of the ASME Computers in Engineering Conf.*, San Francisco, Vol. 1, pp. 465–471 (1992).

APPENDIX A

Planar Curves of Degree 2

Let the equation of a general planar curve of degree 2 be given by

$$ax^2 + by^2 + hxy + px + qy + r = 0$$

The nature of this curve depends on the sign of the following quantity [16]

$$\Delta = ab - \frac{h^2}{4}$$

- if $\Delta > 0$: the curve is an ellipse;
- if $\Delta = 0$: the curve is a parabola;
- if $\Delta < 0$: the curve is a hyperbola.

APPENDIX B

Expression of the Curve of Degree 2 in its Principal Coordinates

Let the singularity locus be given by:

$$E_1x^2 + E_2y^2 + E_3xy + E_4x + E_5y = 0 \tag{B1}$$

For purposes of simplification, let us assume that c_3 is equal to zero which leads to

$$E_1 = -d_3l_2\sin\phi$$

$$E_2 = c_2l_3\cos(\phi + \gamma)$$

$$E_3 = d_3l_2\cos\phi - c_2l_3\sin(\phi + \gamma)$$

$$E_4 = c_2d_3l_2\sin\phi - d_3l_2l_3\cos(\phi + \gamma)\sin\phi - c_2l_2l_3\sin\phi\sin(\phi + \gamma)$$

$$E_5 = -c_2d_3l_3\cos(\phi + \gamma) + d_3l_2l_3\cos\phi\cos(\phi + \gamma) + c_2l_2l_3\cos(\phi + \gamma)\sin\phi$$

The curve can be rewritten as:

$$y_1 = \left(-\frac{E_5 + E_3x}{E_2} + \sqrt{-\frac{4x(E_4 + E_1x)}{E_2} + \frac{(E_5 + E_3x)^2}{E_2^2}}\right)\Big/2$$

$$y_2 = \left(-\frac{E_5 + E_3x}{E_2} - \sqrt{-\frac{4x(E_4 + E_1x)}{E_2} + \frac{(E_5 + E_3x)^2}{E_2^2}}\right)\Big/2$$

The equations of the asymptotes (or of the principal axes) are written as

$$Y_1 = p_1 x + b_1$$
$$Y_2 = p_2 x + b_2$$

with

$$p_1 = \frac{-E_3 + dd}{2E_2}$$
$$p_2 = \frac{-E_3 - dd}{2E_2}$$

and

$$b_1 = \frac{-2E_2E_4 + E_3E_5 - ddE_5}{2E_2 dd}$$
$$b_2 = \frac{2E_2E_4 - E_3E_5 - ddE_5}{2E_2 dd}$$

where

$$dd = \sqrt{-4E_1E_2 + E_3^2}$$

The intersection of the asymptotes (or the principal axes) (x_0, y_0) is obtained as

$$x_0 = \frac{2E_2E_4 - E_3E_5}{dd^2}$$
$$y_0 = \frac{-2E_2E_3E_4 + E_3^2E_5 - E_5dd^2}{2E_2dd^2}$$

Translation of the origin: The origin of the coordinate system is first moved to point (x_0, y_0):

$$x' = x - x_0$$
$$y' = y - y_0$$

Equation (B1) then becomes

$$F + 64E_1^3E_2^3x^2 - 32E_1^2E_2^2E_3^2x^2 + 4E_1E_2E_3^4x^2 + 64E_1^2E_2^3E_3xy - 32E_1E_2^2E_3^3xy + 4E_2E_3^5xy + 64E_1^2E_2^4y^2 - 32E_1E_2^3E_3^2y^2 + 4E_2^2E_3^4y^2 = 0 \quad \text{(B2)}$$

with

$$4E_2dd^4 \neq 0$$

and

$$F = -4E_2(4E_1E_2 - E_3^2)(E_2E_4^2 - E_3E_4E_5 + E_1E_5^2)$$

Rotation of the coordinate system: The new coordinate system is then rotated through an angle η in order to coincide with the principal axes of the curve

$$x' = X\cos\eta - Y\sin\eta$$
$$y' = X\sin\eta + Y\cos\eta$$

Angle η is given by

$$\eta = \frac{\pi}{2} + \frac{\alpha_1 + \alpha_2}{2}$$

where α_1 and α_2 are the angles between the X axis and the asymptotes (or principal axes). The following trigonometric identities are then applied to the resulting equation:

$$\cos\left(\frac{\pi}{2} + \frac{\alpha_1 + \alpha_2}{2}\right) = -\sin\left(\frac{\alpha_1 + \alpha_2}{2}\right)$$
$$\sin\left(\frac{\pi}{2} + \frac{\alpha_1 + \alpha_2}{2}\right) = \cos\left(\frac{\alpha_1 + \alpha_2}{2}\right)$$
$$\sin\left(\frac{\alpha_1 + \alpha_2}{2}\right) = \sqrt{(1 - \cos(\alpha_1 + \alpha_2))/2}$$
$$\cos\left(\frac{\alpha_1 + \alpha_2}{2}\right) = \sqrt{(1 + \cos(\alpha_1 + \alpha_2))/2}$$
$$\cos(\alpha_1 + \alpha_2) = \cos\alpha_1\cos\alpha_2 - \sin\alpha_1\sin\alpha_2$$
$$\sin(\alpha_1 + \alpha_2) = \sin\alpha_1\cos\alpha_2 + \cos\alpha_1\sin\alpha_2$$
$$\cos\alpha_1 = 1/\sqrt{1 + p_1^2}$$
$$\sin\alpha_1 = p_1/\sqrt{1 + p_1^2}$$
$$\cos\alpha_2 = 1/\sqrt{1 + p_2^2}$$
$$\sin\alpha_2 = p_2/\sqrt{1 + p_2^2}$$

where

$$p_1 = \tan \alpha_1$$

$$p_2 = \tan \alpha_2$$

This leads to:

$$H_0 + H_x X^2 + H_y Y^2 = 0 \tag{B3}$$

with

$$\begin{aligned}
H_0 &= 2D_1 D_2 E_2 F \\
H_x &= 64E_1^4 E_2^3 - 128E_1^3 E_2^4 + 64D_1 D_2 E_1^3 E_2^4 + 64E_1^2 E_2^5 + 64D_1 D_2 E_1^2 E_2^5 \\
&\quad - 32E_1^3 E_2^3 E_3^2 + 128E_1^2 E_2^3 E_3^2 - 32D_1 D_2 E_1^2 E_2^3 E_3^2 - 32E_1 E_2^4 E_3^2 \\
&\quad - 32D_1 D_2 E_1 E_2^4 E_3^2 + 4E_1^2 E_2 E_3^4 - 40E_1 E_2^2 E_3^4 + 4D_1 D_2 E_1 E_2^2 E_3^4 \\
&\quad + 4E_2^3 E_3^4 + 4D_1 D_2 E_2^3 E_3^4 + 4E_2 E_3^6 \\
H_y &= -64E_1^4 E_2^3 + 128E_1^3 E_2^4 + 64D_1 D_2 E_1^3 E_2^4 - 64E_1^2 E_2^5 + 64D_1 D_2 E_1^2 E_2^5 \\
&\quad + 32E_1^3 E_2^3 E_3^2 - 128E_1^2 E_2^3 E_3^2 - 32D_1 D_2 E_1^2 E_2^3 E_3^2 + 32E_1 E_2^4 E_3^2 \\
&\quad - 32D_1 D_2 E_1 E_2^4 E_3^2 - 4E_1^2 E_2 E_3^4 + 40E_1 E_2^2 E_3^4 + 4D_1 D_2 E_1 E_2^2 E_3^4 \\
&\quad - 4E_2^3 E_3^4 + 4D_1 D_2 E_2^3 E_3^4 - 4E_2 E_3^6
\end{aligned}$$

where

$$\begin{aligned}
D_1 &= \sqrt{1 + p_1^2} \\
D_2 &= \sqrt{1 + p_2^2} \\
F &= -4E_2(4E_1 E_2 - E_3^2)(E_2 E_4^2 - E_3 E_4 E_5 + E_1 E_5^2)
\end{aligned}$$

Finally, the division of equation (B3) by H_0 gives:

$$1 + \frac{X^2}{H_{0x}} + \frac{Y^2}{H_{0y}} = 0 \tag{B4}$$

with

$$H_{0x} = \frac{H_0}{H_x}$$

$$H_{0y} = \frac{H_0}{H_y}$$

If the coefficients H_{0x} and H_{0y} are both negative, when equation (B4) is the equation of an ellipse and the length of its principal axes are respectively given by:

$$AB_1 = 2\sqrt{-H_{0x}}$$

$$AB_2 = 2\sqrt{-H_{0y}}$$

On the other hand, if H_{0x} and H_{0y} are of opposite signs, then equation (B4) is a hyperbola and the minimum distance between the branches, noted $d_{\min}$, is given by:

$$d_{\min} = 2\sqrt{-H_{0y}} \quad \text{if} \quad H_{0x} > 0 \quad \text{and} \quad H_{0y} < 0; \tag{B5}$$

$$d_{\min} = 2\sqrt{-H_{0x}} \quad \text{if} \quad H_{0x} < 0 \quad \text{and} \quad H_{0y} > 0. \tag{B6}$$

ETUDE DES LIEUX DE SINGULARITÉ QUADRATIQUES DES MANIPULATEURS PARALLÈLES PLANS À TROIS DEGRÉS DE LIBERTÉ

Résumé—Dans cet article, on présente l'étude et la représentation des lieux de singularité dans l'espace de travail cartésien du manipulateur parallèle plan général à 3 degrés de liberté. La méthode utilisée ici est basée sur l'annulation du déterminant de la matrice jacobienne du manipulateur. Dans des travaux antérieurs, trois grands types de singularités ont été identifiés pour les manipulateurs parallèles. On s'intéresse, dans cette étude, aux singularités de type I et II, c'est-à-dire celles pour lesquelles le nombre de solutions au problème géométrique (i) inverse et (ii) direct dégénère. Le 3ième type, appelé aussi singularité architecturelle, est supposé éliminé par un bon choix des paramètres géométriques du manipulateur. En effet, ce type de singularité est facile à prévoir pour le manipulateur étudié ici et les conditions dans lesquelles ces singularités se produisent ont été explicitées ailleurs.

Le travail développé ici aboutit à une expression analytique quadratique pour les singularités de type II. A partir de cette expression, il est montré que le lieu des singularités de ce type, pour une orientation

donnée de la plate-forme, est soit une hyperbole, soit une parabole, soit un ellipse. Des exemples de manipulateurs parallèles plans à 3 degrés de liberté sont traités. Pour chacun des exemples montrés, les courbes de singularité sont superposées à l'espace atteignable du manipulateur grâce à un logiciel de CAO spécialement dédié aux manipulateurs parallèles et dans lequel les expressions développées ici ont été intégrées. Une représentation tridimensionelle des courbes de singularité est aussi donnée. Des cas de manipulateurs ne présentant pas de singularité pour certaines orientations ont été mis en évidence par simulation graphique. Par ailleurs, les singularités de type I sont représentées par les limites de l'espace de travail tracé dans l'espace cartésien et sont donc faciles à obtenir. La représentation graphique des lieux de singularité constitue un outil puissant d'analyse et de conception puisqu'elle permet à l'utilisateur d'avoir très rapidement une excellente idée de la localisation des configurations potentiellement critiques.